Article

Interactions Between Corn Starch and Ethyl Maltol Under Heat-Moisture Treatment and Its Application in Fried Chicken Nuggets

Meijuan Xu , Tianwen Liu , Jianguo Song , Xueqin Gao , Yuran Shi , Xiaodong Zhao , Jian Zou *

Posted Date: 8 October 2024

doi: 10.20944/preprints202410.0484.v1

Keywords: heat-moisture temperature; non-inclusion complex; structure; coating powders

Article

Interactions between Corn Starch and Ethyl Maltol under Heat-Moisture Treatment and Its Application in Fried Chicken Nuggets

Meijuan Xu [1,2], Tianwen Liu [3], Jianguo Song [4], Xueqin Gao [1], Yuran Shi [1], Xiaodong Zhao [1] and Zou Jian [1,*]

[1] College of Food and Biological Engineering, Henan University of Animal Husbandry and Economy, Zhengzhou 450046, China
[2] College of Food Science and Technology, Huazhong Agricultural University; Wuhan 430070, China
[3] School of Life and Health Sciences, Hubei University of Technology, Wuhan 430068, China
[4] Henan Xikang Food Co., LTD, Xinxiang 453000, China
* Correspondence: 81450@hnuahe.edu.cn

Abstract: The study delved into the interaction between corn starch and ethyl maltol during innovative repeated-continuous heat-moisture treatment (RCHMT), and its impact on the quality of fried chicken nuggets. The results revealed that the complexation ratio of ethyl maltol in the corn starch-ethyl maltol complex remained stable, and the complex created dense microporous structures. Native starch and complex samples exhibited an A-type crystal structure, while the physical mixture sample showed a C_a-type. Additionally, the peak of C-O-H def., CH_2 of the complex sample was red-shifted, and the hydrogen bond structure was enhanced. Moreover, the complex exhibited a higher resistant starch content and lower hydrolysis rate than the physical mixture sample. The starch-ethyl maltol formed by RCHMT is a non-inclusion complex. It has been shown to reduce oil absorption and enhance the crispness of fried chicken nuggets, matching that of commercial products. This finding provides a direction for the development of innovative coating powders.

Keywords: heat-moisture temperature; non-inclusion complex; structure; coating powders

1. Introduction

Deep-fried coated food products have gained popularity due to their desirable golden color, satisfying crispy texture and unique flavor, as evidenced by its multi-billion dollar market [1]. However, excessive oil absorption during frying and cooling creates a greasy texture and an unfavorable consumer experience [2]. High-oil absorption products contribute to obesity, cardiovascular disease, and other health issues [2]. Besides, industrial frozen meat in the thawing process causes flavor loss, resulting in fried-coated food products lacking meat flavor [3]. Simultaneously, the reduced crispiness and quick loss of texture are the non-negligible challenges in deep-fried coated food products, which are attributed to the starch type in the coating, the frying process, and freezing procedures [4,5]. Researchers have explored various innovative strategies to address these challenges, such as enhancing crispiness, reducing oil absorption by cross-linked and pregelatinized modified starches [6,7], and improving meat flavor stability by introducing ethyl maltol. Nevertheless, the structure of the cross-linked and pregelatinized modified starches was severely destroyed [7], which limits further modification of starch. The high-temperature instability and extremely volatile limit ethyl maltol's application [8]. Under the premise of maintaining the starch structure, it is important to develop a physical modification technology that combines starch with ethyl maltol, which can not only improve the stability of flavor substances, but also make starch with high crispness and low oil absorption properties.

 doi:10.20944/preprints202410.0484.v1

During food processing, starch forms complexes with ligands such as fatty acids, polyphenols, and flavor compounds [9]. Starch granules swell as they absorb water, causing starch chains to open and twist into hydrophobic helical voids through helical folding under hydrogen bonding, with hydrophobic methylene and glycosidic bonds in the interior and hydrophilic hydroxyl glucose residues on the outside [10,11]. Small ligands entering the helical structure of amylose form V-type crystal structures or left-handed single helical complexes [10], while larger ligands form complexes through hydrogen bonding on the outside of amylose chains [11]. The interaction between starch and ligands relies on non-covalent bonds such as hydrogen bonding, hydrophobic interaction, CH-π bonding, etc. [10,12]. The hydrogen bonding and hydrophobic interactions within the system are crucial in facilitating the complexation process between starch and ligands, leading to significant modifications in the rheological and digestive properties of the starch [13].

Wall materials containing flavor substances include cyclodextrins, starches, hydrophilic colloids and proteins. Among them, starch is the most inexpensive and effective method for encapsulation. Methods for preparing starch-small molecule flavor substance complexes mainly include dimethyl sulfoxide solvent, alkali, zinc chloride, hydrothermal, and ultrasound-assisted preparation methods. The alkali method and zinc chloride solvent method promote the transformation of the starch helical structure into a random coiled shape, thereby enhancing the binding of the helical structure with thymol to form a V-type crystal structure [14]. Still, the chemical methods introduce chemical reagents, contradicting the development trend of "clean label". Hydrothermal methods and ultrasound-assisted hydrothermal methods are significantly affected by hydrothermal conditions, and strict control of water content and processing temperature is required to complex with the ligand [15,16].

Heat-moisture treatment is a hydrothermal physical modification technology. Repeated modification technology involves treating the starch by heating and cooling in cycles and the continuous modification process consists in heating the starch continuously for a certain time. Our previous research found that repeated hydrothermal modification technology can quickly open the spiral structure of the starch and rearrange amylose and amylose/ amylopectin, improving the starch crystalline structure, increasing the helical structure content and decreasing the digestibility [17,18]. Based on this, this study combines repeated heat-moisture treatment with continuous heat-moisture treatment (repeated-continuous heat-moisture treatment, RCHMT) to prepare a starch-ethyl maltol complex sample, analyzes the complexation mechanism of starch and ethyl maltol under this technology, establishes the correlation between structure and digestibility, and finally applies the complex sample to fried coated meat products to explore the effect on the quality of fried chicken nuggets.

2. Materials and Methods

2.1. Materials

Normal corn starch (purity ≥98%) was purchased from Nanjing Huafeikou Alkali Factory Co., LTD. Ethyl maltol (purity ≥99%) and α-amylase (11 u/mg) were obtained from Yuanye Biotechnology Co., LTD. (Shanghai, China). Glucosidase (10^5 u/mL) was purchased from Maclin Biochemical Technology Co., Ltd, and a D-glucose test kit was purchased from Megazyme Co., Ltd. Other chemical reagents were analytically pure. Commercially available chicken nuggets were provided by CP GROUP.

2.2. Sample Preparation and Structure-Digestibility Determination

2.2.1. Preparation of Corn Starch-Ethyl Maltol Complex and Mixture Sample

The factors affecting the complexation ratio of corn starch-ethyl maltol complex prepared by RCHMT were excavated through single factor and response surface tests. Factors such as the water content (factor 1), amount of ethyl maltol (factor 2), cycles of repeated heat moisture (factor 3), and treatment time of continuous heat moisture (factor 4) were well identified. This result is showed in Supplementary document.

 doi:10.20944/preprints202410.0484.v1

The meticulous process of recombination is as follows: The weighted 100.00 g of native corn starch (named for native starch) was accurately weighed and the moisture content was adjusted to 34% with distilled water (factor 1). A portion of the distilled water was used to dissolve 0.40 g of ethyl maltol (factor 2). The mixture was then evenly combined in a blue-capped silk bottle and left to balance at room temperature for 24 hours for subsequent RCHMT. The sample was heated in an oven at 94 °C for 4 hours and allowed to cool naturally at room temperature (25 ± 2 °C) for 1 hour. This step was repeated twice (factor 3) to obtain the repeated heat-moisture treatment sample. Subsequently, the above samples were continuously treated in the oven at 94 °C for 12 hours (factor 4) to get the RCHMT sample. The obtained sample was washed with ethanol-water (1: 1, V: V) three times to remove the free ethyl maltol. Finally, the sample was dried at 45 °C, and crushed through a 100-mesh sieve to obtain the corn starch-ethyl maltol complex (named for the complex sample). The mixture sample before RCHMT was used as the control (named for the mixture sample).

2.2.2. Complexing Ratio

The content of ethyl maltol was determined by High-performance liquid chromatography according to the GB 5009.250-2016. The complex (2 g) was placed into centrifuge tubes, and 5 mL of distilled water and 15 mL of methanol solution were added to each tube for ultrasound treatment for 20 min. Besides, the different ultrasonic time (1 h, 4 h, 8h, 12 h, and 24 h) was investigated to evaluate the stability of the complex. The methanol solution was used to keep a constant volume of 25 mL. The solution was centrifuged (6000 r/min) for 10 min. A microporous filter membrane filtered the supernatant. The ratio of ethyl maltol content from a complex sample to a mixture sample was regarded as the complexation ratio.

2.2.3. Scanning Electron Microscope (SEM)

The sample was secured with conductive double-sided tape. Excess starch was removed by blowing, and then platinum was sprayed and observed under 1000x and 3000x magnification.

2.2.4. X-ray Diffraction (XRD)

X-ray diffraction tests were executed on samples. A precise sample was strategically positioned and continuously scanned on a rectangular aluminum sheet. The tests were conducted employing a copper target, ensuring accuracy and thoroughness within a range of 5° to 50°, at a speed of 6°/min with a step size of 0.02°.

2.2.5. Fourier Infrared (FT-IR)

The sample and KBr were mixed in a ratio of 1:50, ground to a fine powder in a mortar, and then compressed into tablets for determination. The measurement was carried out within the range of 4000 cm^{-1} to 400 cm^{-1}, with 32 scans and a resolution of 4 cm^{-1}. In addition, the Lorenz curve function was deconvolved for the 1200-800 cm^{-1} region using OMNIC software, with a half-peak width of 32 cm^{-1} and a factor of 1.9.

2.2.6. ^{13}C Solid State Nuclear Magnetic Resonance (^{13}C-NMR)

The sample was placed in a rotor and analyzed using a 599.7 MHZ wide-cavity solid superconducting NMR spectrometer with a 7 mm MAS BB/BB probe at a MAS speed of 12 kHz.

2.2.7. Differential Scanning Calorimetry (DSC)

For the DSC analysis, 3 mg of the sample was evenly spread in an aluminum dish and mixed with 9 μL of ultra-pure water. After tightly sealing the dish, it was kept at room temperature overnight for equilibration. The temperature was then measured with a heating rate of 10 °C/min within the range of 30 °C to 150 °C.

2.2.8. Digestible Components of Starch

 doi:10.20944/preprints202410.0484.v1

According to the method of Zou et al (2023) [19], 50 mg of starch and 10 mL of phosphate buffer (0.5 mol/L, pH=5.2) were thoroughly mixed and then incubated at 37 °C for 10 min. After that, 4 mL of porcine pancreatic alpha-amylase (3000 U/mL) and 1 mL of starch glucosidase (2500 U/mL) were added to the starch paste. The mixture was then incubated at 37 °C for 0, 10, 20, 30, 60, 90, 120, 150, and 180 min. After each time point, 0.5 mL of Na_2CO_3 (0.3M) was added to the hydrolysate to deactivate the enzyme. Following centrifugation at 5000 r/min for 10 min, 0.1 mL of the supernatant was combined with 3 mL of GOPOD reagent for glucose content analysis. The glucose content at 20 and 120 min was utilized to calculate the RDS, SDS, and RS content.

$RDS(\%)=(G_{20}-G_0)/W*0.9*100$

$SDS(\%)=(G_{120}-G_{20})/W*0.9*100$

$RS(\%)=1-RDS-SDS$

2.2.9. First-Order Kinetic Fitting

The digestibility can be fitted to first-order kinetics according to the method from Zou et al. (2023) [19]. The first-order kinetic equation is:

$C_t=C_\infty$ (1-e^(-kt))

Where:

$C_t(\%)$: the percentage of starch digested in time t (min);

$C_\infty(\%)$: the estimated percentage of starch digested at the end of the reaction;

$K(min^{-1})$: digestion rate coefficient, estimated by transforming the equation using slope analysis (LOS).

$ln(dc/dt)=-kt+ln(C_\infty K)$

Where: ln(dc/dt) represents the logarithm of the slope, and this equation describes the linear relationship between LOS and starch hydrolysis time.

2.3. Application of Complex in Refried Chicken Nuggets

2.3.1. The Preparation of Coating Powder

Preparation of original coating powder: wheat flour: potato starch: sweet potato starch =1:5:5 (w/w/w).

Preparation of composite coating powder: The original coating powder was replaced with a complex in varying proportions (0%, 3%, 6%, 9%, 12% and 15%).

2.3.2. Preparation of Refried Chicken Nuggets

The weighted chicken breast was cut into 1 cm^3 pieces (the weighing was labeled M_0) and combined with the composite coating powder. After a brief water soak (10 s) and two coatings (the weighing was labeled M_1), the samples were fried at 170 °C for 4 min (the weighing was labeled M_2), then cooled and freeze-dried at -40 °C for 48 hours. The frozen pre-fried chicken pieces were refried at 180 °C for 1.5 min. The M_0, M_1, and M_2 were used to calculate the following coating pick-up and oil absorption ratio.

2.3.3. Coating Pick-Up and Oil Absorption Rate

The pick-up of the chicken nuggets was defined as the ratio of coating weight to the total chicken breast weight before coating:

$Pick\text{-}up(\%)=(M_1-M_0)/M_0*100\%$

Where: M_0 was the chicken breast weight; M_1 was the weight of the coated chicken breast.

The oil absorption rate was defined as the ratio of oil absorption weight to the weight of the coated chicken breast.

$Oil\ absorption\ ratio(\%)=(M_1-M_2)/M_1*100\%$

Where: M_1 was the weight of the coated chicken breast. M_2 was the weight of the fried coated chicken breast.

 doi:10.20944/preprints202410.0484.v1

2.3.4. Texture Test

The specific parameters for texture analysis were as follows: TA41 probe was selected, the pretest, test, and return speeds for compression testing were all 1 mm/s, the load trigger force was 5 g, and the strain value was 50%. Each sample was tested five times.

2.3.5. Colors

The color of the samples was meticulously measured using a high-precision spectrophotometer to obtain L*(Lightness), a*(red), b*(yellow) and △E values. Each group of samples was meticulously measured 6 times in parallel. L_0*, a_0*, b_0* referred to the color value of the whiteboard. △E is the total color difference:

2.3.6. Sensory Evaluation

Before conducting sensory evaluations, eight evaluators underwent standardized training to assess sensory indicators. Evaluators were strictly prohibited from commucating with one another during the evaluation process. The color, crispness, surface structure, palatability (suitable greasiness), flavor, and comprehensive evaluation of chicken nuggets were evaluated. Ratings varied from 0-10, with 0-4 being the worst, 5-7 moderate, and 8-10 best.

2.4. Data Analysis

Minitab 19 and Origin 2024 software were used to analyze the experimental data and make charts, and each data was repeated three times to obtain the average value.

3. Results and Discussions

3.1. Structure-Digestibility Analysis of Starch-Ethyl Maltol Samples

3.1.1. Analysis of Complexation Ratio

To investigate the effect of ethyl maltol embedding, the complex sample was treated by ultrasound at different times to obtain the percentage of ethyl maltol released. Figure 1 illustrates that with the extension of ultrasonic time, there was no significant difference in the complexation ratio, especially after ultrasonic treatment for 4 h, no more ethyl maltol was released (Figure 1). This also demonstrates that the structure of the complex was stable and could not release more ethyl maltol even if a long enough ultrasonic time was provided.

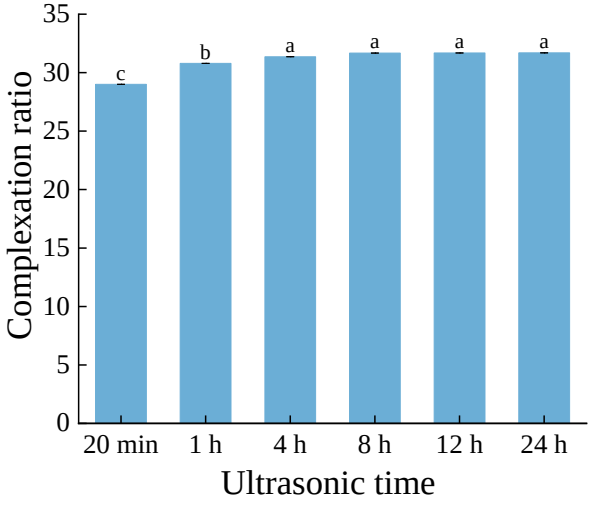

Figure 1. Complexation ratio at different ultrasonic times of the complex sample.

 doi:10.20944/preprints202410.0484.v1

3.1.2. Morphology Observation

The analysis in Figure 2 provides clear evidence of the diverse shapes presented on the surface of native corn starch, including balls, cylinders, ellipsoids, and irregular shapes (Figure 2A). When combined with ethyl maltol without RCHMT, the starch surface exhibited minimal indentation, preserving its overall structure (Figure 2B). When treated by RCHMT, the granule surface of the complex sample did not gelatinize and had dense pores, providing a pathway for entering ethyl maltol into the starch inner structure (Figure 2C). Red adzuki bean starch and rice starch present a coarse or indented granule surface, and even have the aggregate phenomenon induced by heat moisture treatment [20,21]. However, the dense porous surface features resulting from heat-moisture treatment have not been reported. This suggested that RCHMT may be a vital modification technique that made it possible for ethyl maltol to enter the internal structure of starch. Generally, starch granules' surface characteristics significantly impact the enzymatic desensitization and enzymatic hydrolysis mode of α-amylase, leading to substantial changes in starch digestibility [20].

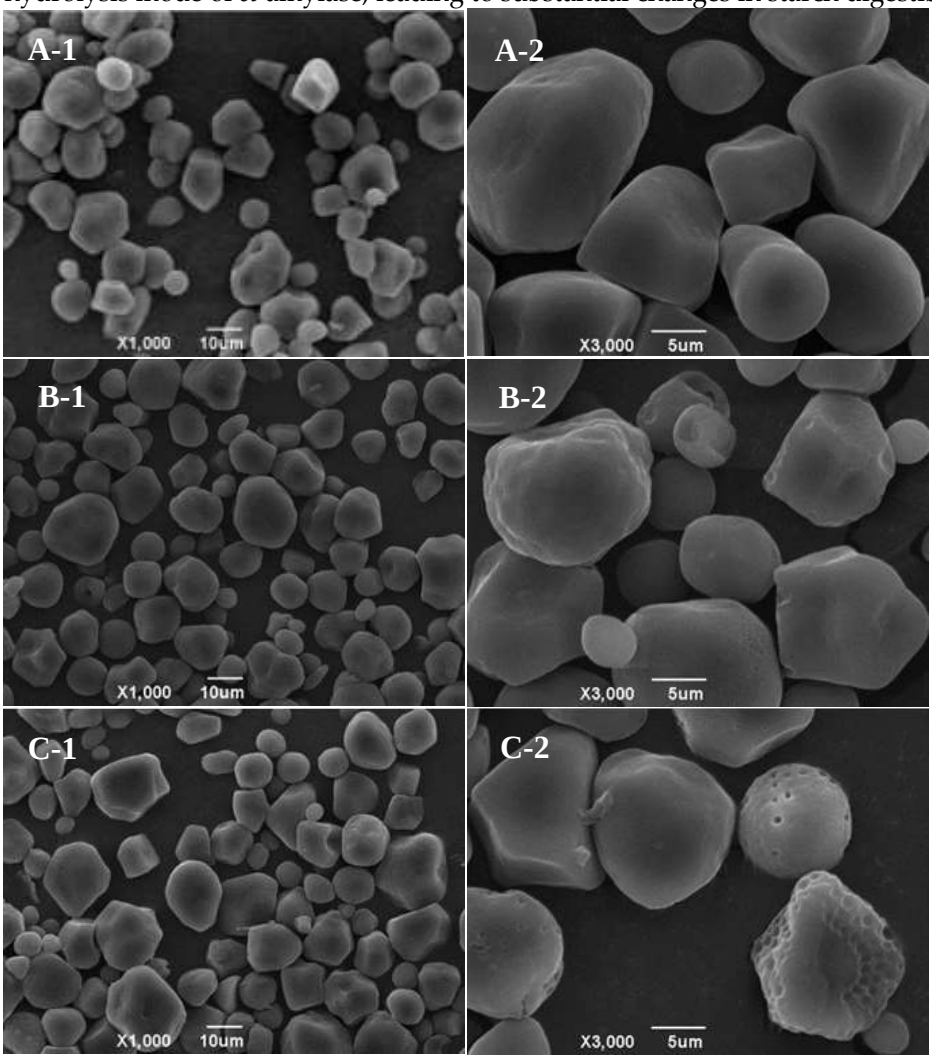

Figure 2. SEM pictures of native starch, mixture and complex samples. A, Native starch; B, Mixture Sample; C, Complex Sample. -1, 1000 magnification; -2, 3000 magnification.

3.1.3. Long-Range Ordering Analysis

In Figure 3A, the distinctive diffraction pattern of ethyl maltol revealed narrow and prominent lines. Meanwhile, the diffraction pattern of native starch presented four sharp peaks at 2θ angles of 15°, 17°, 18°, and 23°, indicative of an A-type crystal structure[18]. Upon mixing, the diffraction pattern stacked the original peaks of ethyl maltol and starch, manifesting double peaks at 22° and 24°

 doi:10.20944/preprints202410.0484.v1

(Figure 3A), suggesting a C-type crystal structure. Hence, this implied that the straightforward physical mixing of starch and ethyl maltol is how ethyl maltol is adsorbed to the surface of starch.

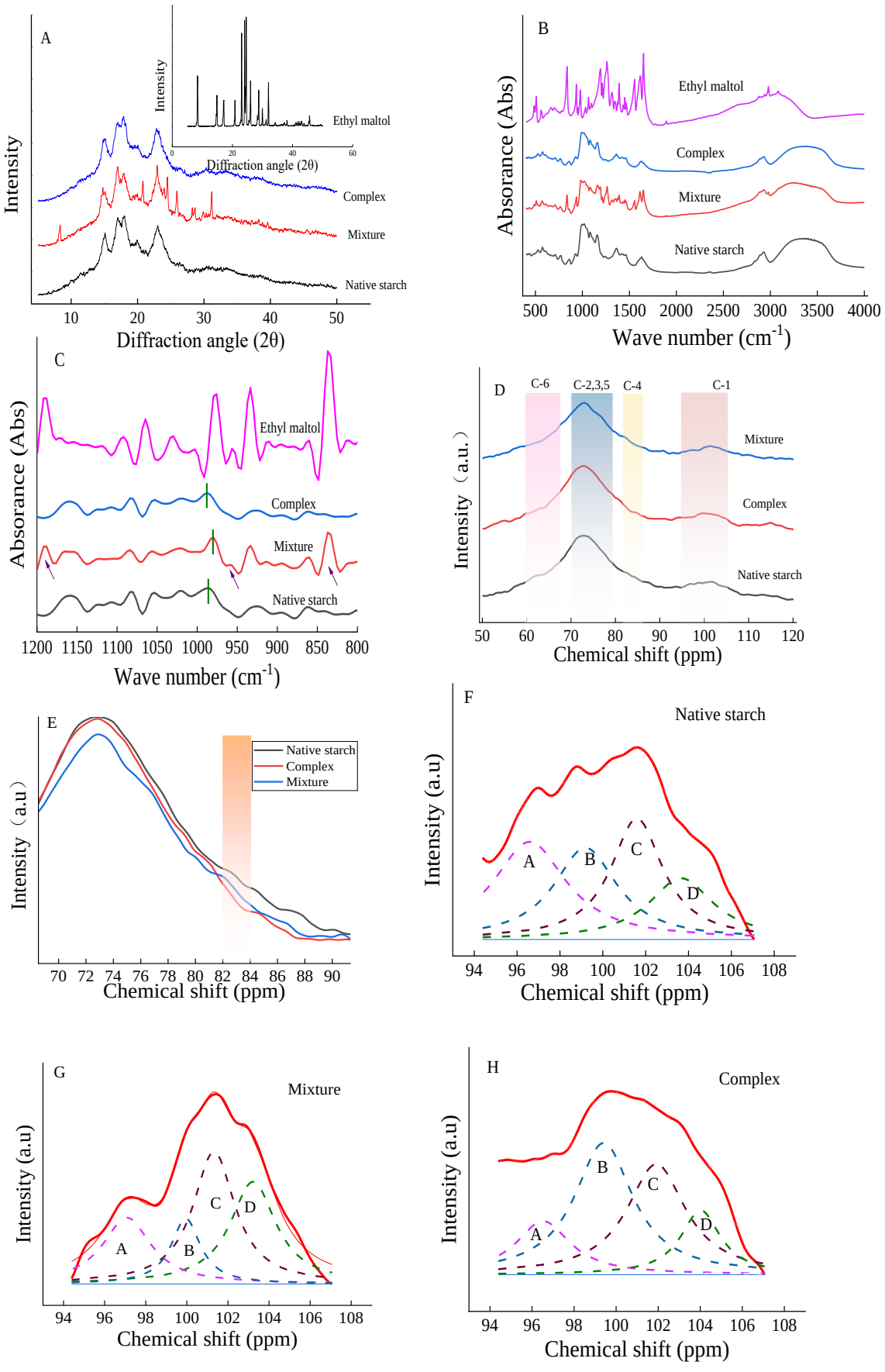

 doi:10.20944/preprints202410.0484.v1

Figure 3. The XRD patterns (A), infrared spectrum (B), infrared deconvolution (C), and ^{13}C-NMR spectra (D-H). E, locally enlarged image of 13C-NMR spectra; F-H, the fitting image in C1 regions of 13C-NMR spectra.

The overall structure of the complex remained A-type (Figure 3A), with no peaks of ethyl maltol detected. This suggests that the combination of starch and ethyl maltol by RCHMT formed a non-covalent bond rather than a covalent bond. This was again confirmed in the FT-IR spectra in Figure 3B-C and NMR in Figure 3D. The formation of inclusion complexes occurs as ligands enter the spiral cavity of starch. Researcher found that the resulting crystal structure exhibits a V-type, altering the original crystalline type [10]. Conversely, non-inclusion complexes are created through straight-side chain connections, with no change to the crystalline type [11]. In general, if ligands are not in the spiral cavity of starch, they form molecular aggregates with starch through hydrogen bonding, hydrophobic interaction and electrostatic interaction[11]. Consequently, the complex's original crystal structure (A-type) persisted even after RCHMT, indicating that ethyl maltol combines with the external side of the starch straight chain through a non-covalent bond to form a non-inclusion complex. The strengthened hydrogen bonding of the complex also improved the relative crystallinity (Table 1).

3.1.4. Short-Range Ordering Analysis

Figure 3B shows that the mixture increased the number of infrared absorption peaks compared to native starch. This indicated that the infrared absorption peaks of ethyl maltol were physically combined with native starch. Fourier infrared deconvolution revealed new absorption peaks at wave numbers 1180, 958, and 895 cm^{-1} in the mixture, which were absent in the complex. This also suggests that only non-covalent bonds rather than covalent bonds were bound in the complex sample.

The vibration absorption peak of C-O-H near 988 cm^{-1} is related to the hydrogen bond on C6 of the starch molecular chain and the dehydrated glucose unit [22]. The peak of the native starch was at 986 cm-1, and the peak of the mixture shifted to a lower wave number (980 cm^{-1}) (Figure 3C), indicating interference with the hydrogen bond structure of corn starch by ethyl maltol. Once the sample was treated by RCHMT, the -OH peak redshifted to a higher wave number, showing that non-covalent bonds (hydrogen bonds) between starch and ethyl maltol were strengthened. $R_{1053/1020}$ represents the short-range order of starch [17]. In Fourier infrared deconvolution Table 1, the short-range order of the mixture decreased. At the same time, that of the complex increased, indicating that RCHMT helped to rearrange the crystal structure of the complex. The short-range order also significantly correlated with starch resistance to digestion (Figure 4E).

Table 1. ^{13}C-NMR parameters of native starch, mixture and complex samples [a].

Samples	C-O-H def., CH2	$R_{1053/1020}$	RC	Peaks	Chemical shift (ppm)	Area ratio (%)
Native starch	986	1.96±0.04[b]	20.06±0.01[a]	$Peak_A$	96.5	27.44
				$Peak_B$	99.1	26.10
				$Peak_C$	101.5	29.39
				$Peak_D$	103.6	17.06
Mixture	980	1.29±0.03[c]	18.45±0.01[c]	$Peak_A$	97.7	19.56
				$Peak_B$	99.9	13.32
				$Peak_C$	101.3	36.98
				$Peak_D$	103	30.12
Complex	988	2.60±0.02[a]	22.50±0.01[b]	$Peak_A$	96.5	13.54
				$Peak_B$	99.4	39.58
				$Peak_C$	101.9	33.38
				$Peak_D$	104.0	13.33

[a] Data within a column having different letters were significantly different ($p < 0.05$).

 doi:10.20944/preprints202410.0484.v1

3.1.5. ^{13}C Solid-State NMR Analysis

The ^{13}C solid-state NMR analysis can provide valuable information about the molecular structure of a sample by revealing changes in chemical shifts. Nuclear magnetic resonance spectroscopy categorizes chemical shifts into four regions (C_1, C_4, $C_{2, 3, 5}$, C_6) based on the properties of the carbons (Figure 3D). Peak resonances at 60-67, 70-79, 82-84, and 94-105 ppm are associated with C_6, $C_{2,3,5}$, C_4, and C_1 carbons, respectively [23]. Specifically, peaks around 103 ppm correspond to the amorphous region of starch, peaks near 100 ppm are linked to a double helix or quasicrystal structure, and peaks at 96.7 ppm and 94.5 ppm are connected to less favorable configurations of starch [24]. In the C_4 region, the peak intensities can serve as indicators of changes in the amorphous composition of starch and a stronger signal in the C_4 region suggests a higher content of the amorphous region [25]. In Figure 3E, the peak intensity of the C4 region of native starch was the greatest, indicating a larger proportion of amorphous regions. Moreover, the peak intensity in the 82-84 ppm range was weaker than that of the native starch and the mixture (Figure 3E), indicating that the proportion of the amorphous zone was decreased due to RCHMT.

To understand the interaction between ethyl maltol and starch after RCHMT, the focus was on the peak treatment of the C_1 region (Figure 3F-H). Analysis revealed three distinct peaks between 100 and 105 ppm in the C1 region of both the native starch and the mixture, indicating that the sample formed an A-type double helix structure after three refolds, which aligns with the crystal structure findings from XRD (Figure 3A). C-type is a mixture of A-type and B-type starch and presents double or triple peaks in the C_1 region [26]. Combined with the results of XRD, the mixture displayed three fitting peaks, signifying that the mixture crystal was C_a-type, mainly an A-type structure. Additionally, the results from Table 1 demonstrated that the order of peak area near 100 ppm ($Peak_B$) was complex >native starch > mixture, showing that the crystallinity of the complex improved after RCHMT, in line with the RC results (Table 1). The $Peak_B$ area has a highly positive correlation with RC in Figure 4E.

3.1.6. Thermal Properties Analysis

The phase transition starting temperature is denoted as T_o, the peak temperature is T_p, and the final value temperature is T_c. Table 2 showed that the complex's T_o, T_p, and T_c were higher than native starch. This indicates a potential increase in the pasting phase transition temperature due to the strengthened hydrogen bonds formed by amylose and ethyl maltol. A positive relationship between hydrogen bonds and thermal parameters is presented in Figure 4E.

Table 2. Thermal parameter, starch components and hydrolysis parameter of native starch, mixture and complex samples [a].

	Parameters	Native starch	Mixture	Complex
Thermal parameters	T_o (°C)	65.05±1.77[b]	66.35±0.07[b]	74.30±0.42[a]
	T_p (°C)	74.55±0.50[b]	74.55±0.35[b]	108.32±0.12[a]
	T_c (°C)	77.40±0.71[b]	76.98±0.30[b]	115.69±0.20[a]
	ΔH/(J/g)	9.28±0.07[b]	8.97±0.09[b]	13.31±0.16[a]
Starch components	RDS	39.83±1.15[b]	43.42±0.56[a]	28.97±1.32[c]
	SDS	21.67±1.40[a]	23.14±0.53[a]	23.13±0.33[a]
	RS	38.5±0.31[b]	33.44±0.84[c]	47.9±1.11[a]
Hydrolysis parameters	K_1	0.090±0.001a	0.081±0.006[a]	0.078±0.006[a]
	$C_{1\infty}$	50.08±1.110[b]	58.67±3.071[a]	37.33±1.590[c]
	K_2	0.037±0.006[a]	0.041±0.010[a]	0.024±0.001[a]
	$C_{2\infty}$	60.05±1.680[b]	67.88±0.094[a]	55.32±0.153[c]

[a] Data within a line having different letters were significantly different ($p < 0.05$).

The gelatinization enthalpy (ΔH) is associated with the double helix structure of starch and its crystal state [19]. The complex exhibited a larger gelatinization enthalpy compared to the mixture due to the presence of intermolecular interactions. This implies that more energy is required to disrupt its spiral structure [17], indicating a relatively strong compound effect. In general, the thermal

 doi:10.20944/preprints202410.0484.v1

stability of the complex was greatly improved, that is, the ethyl maltol required higher energy to be released. ΔH had a positive correlation with the RC, $Peak_B$ area, and RS content and a negative correlation with the hydrolysis parameter (Figure 4E).

3.1.7. Starch Components Analysis

Table 2 shows the results of rapidly digestible starch (RDS), slowly digestible starch (SDS), and resistant starch (RS). The RS content in the mixture decreased compared to native starch. This could be due to ethyl maltol interfering with the short-range order of the starch, making it more easily broken down by the enzyme amylase. Figure 4E also proved that RS had a positive correlation with short-range order and a negative correlation with the hydrolysis parameters. The RS content of the complex significantly increased after RCHMT. Generally, the microporous structure or degradation of starch granules help increase the sensitivity of amylase and improve starch digestibility [27,28]. In theory, the porous structure of the surface of the complex sample helped to improve the digestibility, but the results contradict this, further confirming that the hydrogen bond formed between corn starch and ethyl maltol strengthens the starch structure and reduces the enzyme sensitivity. In the combination of starch-ferulic acid, the strengthened hydrogen bond between the two compounds has also been confirmed to reduce the digestibility of amylase [29]. Therefore, regulating water and temperature in food processing to combine food raw materials with ligands (fat, flavor substances, polyphenols, etc.) is an important research direction for reducing the digestibility of starch and regulating blood sugar.

3.1.8. First-Order Kinetic Analysis

The LOS is utilized to analyze the hydrolysis kinetics of samples, revealing a two-phase hydrolysis process (Figure 4B-D). The initial rapid phase, occurring 30 min before digestion, was followed by a slower or constant phase (Figure 4B-D). Two sets of first-order kinetic constants (K_1, K_2) and percentage hydrolysis ($C_{1\infty}$, $C_{2\infty}$) were obtained, and K and C∞ refer to the rate of enzymatic hydrolysis during digestion and the end-stage percentage of hydrolysis. Consistently, the K value of the first phase surpassed that of the second phase, attributable to the removal of quickly digestible starch during the rapid hydrolysis, leaving only starch less sensitive to the enzyme [30]. Additionally, the K value and hydrolysis percentage of the complex sample were notably smaller than those of the native starch and mixture (Table 2). The presence of ethyl maltol tightened the internal structure through hydrogen bonding, reducing the enzyme sensitivity of the complex starch, similar to the effects observed in the complex of starch and polyphenols [31].

Furthermore, studies have shown that porous starch granules enhance overall digestibility by allowing enzymes to interact with the surface structure [27]. Despite the porous structure of the complex, this did not lead to improved enzyme digestibility. The reduced starch digestion in the complex may be attributed to the non-covalent interaction of the starch molecular structure in the presence of ethyl maltol, altering the hydrogen bonds of the starch chains and ultimately stabilizing and reducing glucose release.

Preprints.org (www.preprints.org) | NOT PEER-REVIEWED | Posted: 8 October 2024 doi:10.20944/preprints202410.0484.v1

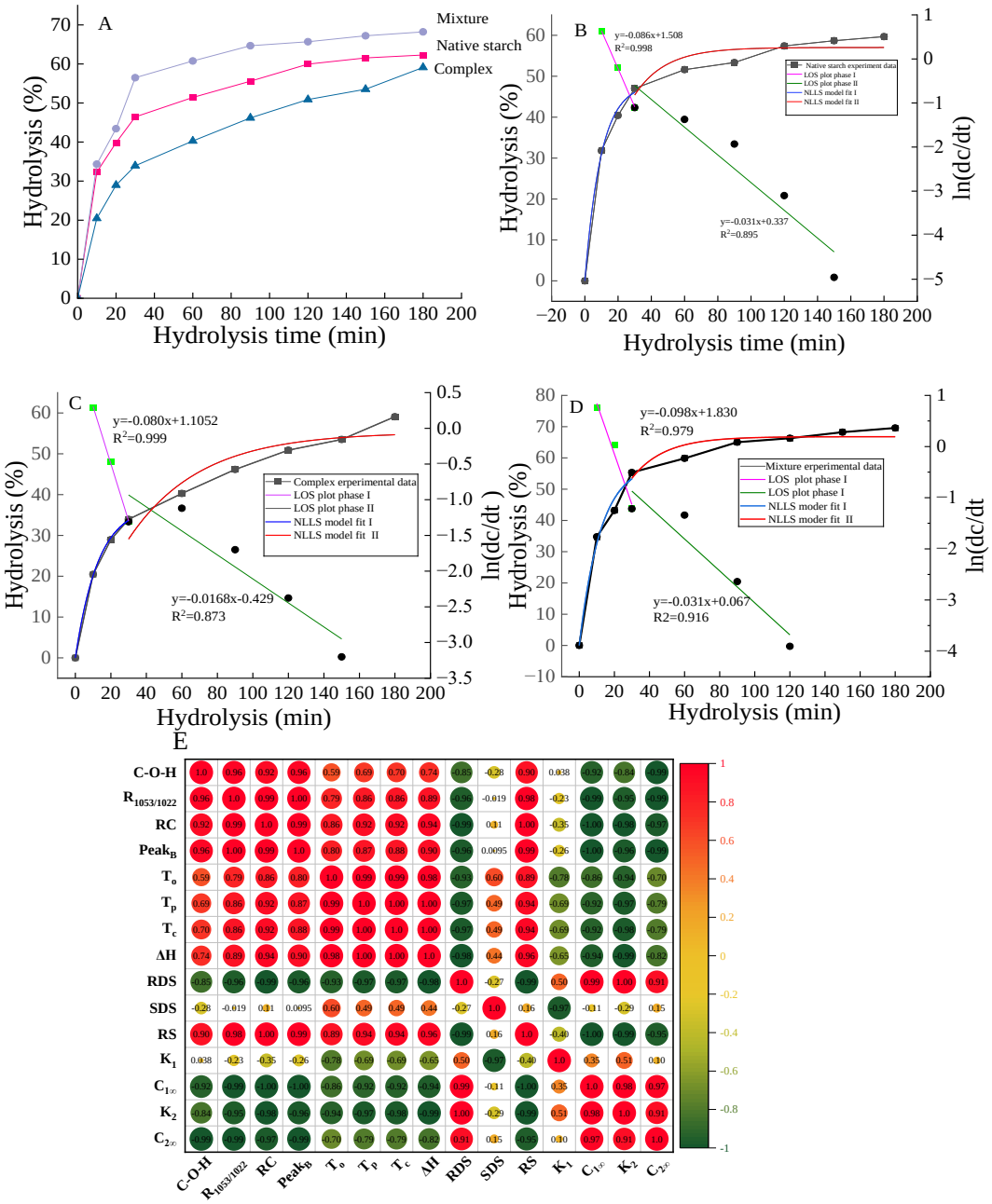

Figure 4. The hydrolysis curves (A), model-fit curves, LOS plots (B-D), and correlation diagram (E) of native starch, mixture and complex samples. E, the correlation analysis was performed by Pearson's correlation analysis.

3.2. Application of Complex in Pre-Fried Chicken Pieces

3.2.1. Coating Pick-Up and Oil Absorption Rate of Chicken Nuggets Prepared by the Complex with Different Addition Ratio

Coating pick-up is an important indicator for fried food, affecting its quality and production rate. The main components of traditional coating powder are wheat flour and starch [1]. The impact of this complex on the coating pick-up is evaluated. Without the addition of the complex, the coating pick-up of the sample was 23.8% (Figure 5A). As the complex was added, the thickness slightly increased, with no significant difference when the complex addition ratio interval was 3%, but a significant difference when the ratio interval was 6% (Figure 5A). Generally, amylopectin is prone to

 doi:10.20944/preprints202410.0484.v1

water absorption and swelling [32]. The addition of the complex increased the coating pick-up, indicating that the complex powder contained a higher amylopectin content. This was because the amylose was combined with ethyl maltol during the RCHMT process, resulting in a decrease in amylose content and an increase in amylopectin content.

The oil absorbance ratio is an important indicator for evaluating the quality of fried products. The structure and properties of starch are key factors determining fried food's oil absorption and texture. The variation in starch oil absorption is related to the granule morphology, crystalline properties, double helix structure, and molecular properties of starch [33]. When no complex was added, the oil uptake was high, but once the complex was introduced, the oil uptake was significantly reduced (Figure 5A). Theoretically, the surface pore structure could increase oil absorption [34], but the oil uptake decreased in reality. Therefore, it is speculated that ethyl maltol entered the hydrophobic helical structure of the starch under RCHMT, hindering the permeating of oil. Meanwhile, the hydrogen bond structure formed by amylose and ethyl maltol strengthened the starch crystal structure, limiting further oil penetration. The addition of resistant starch can also reduce oil uptake [35]. The higher RS content in the complex provides the possibility of a low oil absorption ratio.

3.2.2. Colors of the Chicken Nuggets Prepared by the Complex with Different Addition Ratio

Color is a crucial element in determining the perceived quality of food. When subjected to high-temperature frying, starch undergoes various physical and chemical changes such as dehydration, starch gelatinization, protein denaturation, and the Maillard reaction [36]. These changes significantly impact the oil absorption ratio and color transformation. With an increase in the proportion of the complex sample, the Chicken nuggets showed a decrease in the a* value and an increase in the L* and b* value (Figure 5B), resulting in a yellowish-brown appearance due to heightened color absorption from pigments generated by the Maillard and caramelization reactions [6]. The overall color difference may stem from temperature and moisture content changes, triggering non-enzymatic brownings like the Maillard reaction and caramelization [37]. Compared with the native starch, the total color value exhibited a significant change post-compound addition (Figure 5B). However, the total color difference did not change with the increase of complex addition. This emphasized the complex's capacity to reliably transform the product's color.

3.2.3. Texture of the Chicken Nuggets Prepared by the Complex with Different Addition Ratio

Texture is a vital aspect of quality measurement, and crispness is a highly desirable trait. Different proportions of complexes were added to chicken nuggets to detect the effect on the product's texture. The hardness, adhesiveness, and chewiness increased as the complex proportion increased, while the fracture force decreased overall, especially at 6% (Figure 5C). Some researchers have positively linked hardness with crispness [2], while others have discovered an inverse relationship between hardness and crispness [38]. From a sensory perspective, hardness and crispness are distinct sensory properties. A sample with greater hardness is more challenging to break, while a sample with greater crispness is more likely to break. Fracture force is commonly used to indicate brittleness, representing the peak of the TPA force with the first breaking point on the distance curve. A lower fracture force indicates a crisper specimen [6]. The fracture force initially decreased and then increased with an increase in complex proportion. Hence, 6% is the crucial addition for achieving the perfect crispy chicken nuggets.

 doi:10.20944/preprints202410.0484.v1

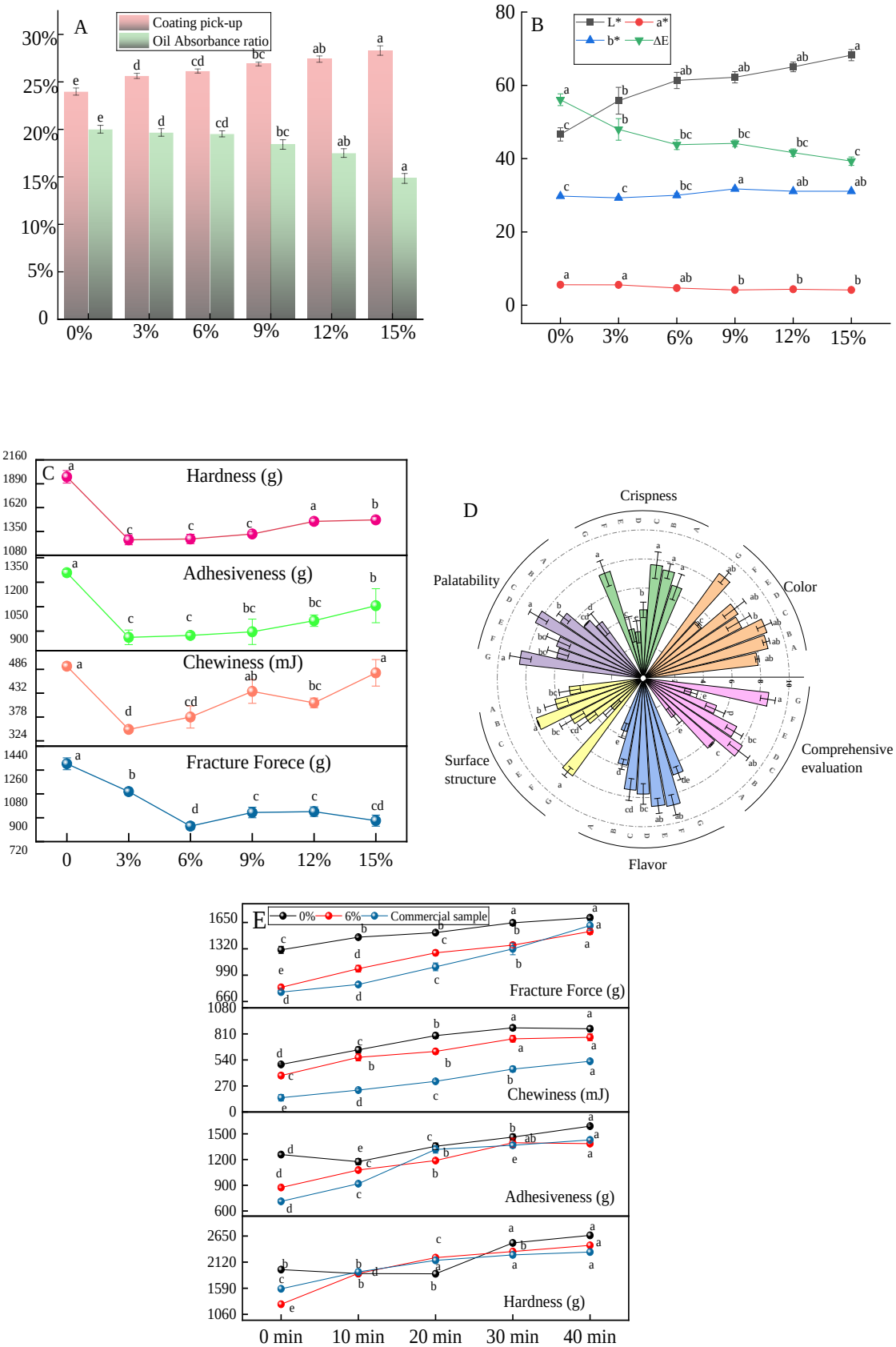

Figure 5. Coating pick-up (A), oil absorption ratio (A), color values (B), texture (C), rose diagram of artificial sensory evaluation (D) of the Chicken nuggets prepared by the complex with different addition ratios, and the texture (E) of chicken nuggets placed at frying different times. In the rose

 doi:10.20944/preprints202410.0484.v1

diagram of artificial sensory evaluation (D), the letters A-F were the samples prepared by the complex with different addition ratios (0%, 3%, 6%, 9%, 12% and 15%), and the letter G was the commercial sample. The lowercase letters were significantly different ($p < 0.05$).

3.2.4. Sensory Evaluation of the Chicken Nuggets Prepared by the Complex with Different Addition Ratio

With the increase of the complex proportion (0%-12%), there was no obvious difference in the observation of human vision, but an unpleasant dark color occurred when the complex was introduced at a ratio of 15% (Figure 5D). The greater the proportion of complex added, the more difficult the crispness to be accepted by consumers. However, as the proportion of complex increased, the meat flavor showed an increasing trend, mainly due to the higher proportion of complex containing more ethyl maltol (Figure 5D). At the same time, the comprehensive sensory scores of the commercial products had no statistical difference compared to that of the chicken nuggets with 6% complex addition (Figure 5D). It's important to note that when the compound powder ratio is 9%, it results in the best palatability. Lower amounts of added powder lead to higher oil absorption and poorer palatability, while higher amounts reduce oil absorption, leading to a lack of smell saturation brought by the oil. Overall, the quality of commercially available chicken nuggets is comparable to that of the complex products.

3.2.5. Comparison of the Texture of Chicken Nuggets Placed at Frying Different Times

There is a prevalent issue in the market where chicken nugget products quickly lose their crispiness after frying. This not only diminishes the overall sensory experience for consumers but also restricts the potential growth of deep-fried products. A study was conducted to analyze the texture changes of chicken nuggets with an optimal complex addition ratio compared with the control sample and commercial products. The results revealed that the addition of the complex sample could effectively regulate the crispiness of the chicken nuggets for an extended period (Figure 5E), matching the quality of commercially available products. The enhanced hydrogen bonding between starch and ethyl maltol might be an important reason for a long-lasting crispy texture. This unique combination makes the starch resistant to enzymatic breakdown and boosts the resistant starch content. Resistant starch has better expansibility and solubility, making the batter puffier and crisper after frying [35]. This breakthrough enables us to offer products that maintain their crispness over time, ultimately enhancing the consumer experience and driving the rapid development of deep-fried coated products.

4. Conclusions

The study aimed to prepare a corn starch-ethyl maltol complex using RCHMT, with native starch and corn starch-ethyl maltol mixture as controls. The results showed that the ethyl maltol in the complex was stable and not easily released. Additionally, a compact microporous structure was formed on the complex's surface. Analysis of the crystal structure and peak fitting in the C_1 region revealed that the complex had an A-type crystal structure, while the mixture had a C_a-type structure, with the amorphous region of the complex being the smallest. FT-IR results showed that hydrogen bond positions in the complex were redshifted, but the mixture showed a blue shift. The thermal parameters and resistant starch of the complex increased, and the hydrolysis was divided into two stages by LOS fitting. In conclusion, a non-inclusion complex was formed by starch and ethyl maltol after RCHMT, mainly through the hydrogen bond structure formed by amylose and ethyl maltol. Subsequently, different proportions of the complex were added to chicken nuggets, and a 6% addition resulted in the highest crispness, best palatability, and better sensory score. In comparison with commercial chicken nuggets, the overall texture was found to be comparable.

Therefore, RCHMT can provide a new method for synthesizing a stable corn starch flavor complex. The results of this study lay a foundation for analyzing the interaction mechanism between corn starch and flavor substances, and also provide ideas and references for the development of powder coating products.

 doi:10.20944/preprints202410.0484.v1

Supplementary Materials: The following supporting information can be downloaded at the website of this paper posted on Preprints.org.

Author Contributions: Author Contributions: Writing-review & editing, M.X.; Methodology, T.L.; Resources, J.S.; Software, X.G.; Validation, Y.S.; formal analysis, X.Z.; Conceptualization, J.Z. All authors have read and agreed to the published version of the manuscript.

Funding: The research was funded by the Key Disciplines of Henan Province (2023-2027) (Number 311, Code 0951), Henan Provincial School-enterprise R&D Center: High Value Utilization of Livestock and Poultry By-Products, K3050004, Education Technology [2024] No. 147 and Science and Technology Research and Development Plan of Henan Province (232102110138).

Institutional Review Board Statement: Not applicable.

Informed Consent Statement: Not applicable.

Data Availability Statement: The original contributions presented in the study are included in the article, further inquiries can be directed to the corresponding author.

Conflicts of Interest: Author Jianguo Song was employed by the company Henan Xikang Food Co., LTD. The role of the company was to provide the resource. The remaining authors declare that the research was conducted in the absence of any commercial or financial relationships that could be construed as a potential conflict of interest.

References

1. Bhuiyan, M.H.R.; Ngadi, M. Application of batter coating for modulating oil, texture and structure of fried foods: a review. Food Chem. **2024**, 453, 13965.
2. Liberty, J.T.; Dehghannya, J.; Nngadi, M.O. Effective strategies for reduction of oil content in deep-fat fried foods: A review. Trends Food Sci Tech. **2019**, 92, 172-183.
3. Hu, R.; Zhang, M.; Liu, W.; Mujumdar, A. S.; Bai, B. Novel synergistic freezing methods and technologies for enhanced food product quality: a critical review. Compr Rev Food Sci Food Saf. **2022**, 21, 1979-2001.
4. Zhang, Y.; Zhang, T.; Fan, D.; Li, J.; Fan, L. The description of oil absorption behavior of potato chips during the frying. LWT-food Sci Technol. **2018**, 96, 119-126.
5. Chen, C.L.; Li, P.Y.; Hu, W. H.; Lan, M. H.; Chen, M. J; Chen, H. H. Using HPMC to improve crust crispness in microwave-reheated battered mackerel nuggets: Water barrier effect of HPMC. Food Hydrocoll. **2008**, 22, 1337-1344.
6. Wang, X.; Mcclements, D.J.; Xu, Z.; Meng, M.; Qiu, C.; Long, J.; Jin, Z.Y.; Chen, L. Preparation and characterization of calcium-binding starch and its application in microwaveable pre-fried foods. Food Hydrocoll. **2024**, 156, 110328.
7. Primo-Martin, C. Cross-linking of wheat starch improves the crispness of deep-fried battered food. Food Hydrocoll. **2012**, 28, 53-58.
8. Zou, P.; Zhang, S. Y.; Jia, L. Y.; He, Z. Y.; Shu, J.; Liu, C. H.; Zhu, Y. Y. A study on the release behavior of ethyl maltol during pyrolysis of its metal complexes. Thermochim Acta **2022**, 176, 179323.
9. Wang, R.; Li, M.; Brennan, M.; Dhital, S.; Kulasiri, D.; & Brennan, C.; Guo, B. Complexation of starch and phenolic compounds during food processing and impacts on the release of phenolic compounds. Compr Rev Food Sci F. **2023**, 22, 3185-3211.
10. Obiro, W.C.; Ray, S.S.; Emmambux, M.N. V-amylose Structural Characteristics, Methods of Preparation, Significance, and Potential Applications. Food Rev Int. **2012**, 28, 412-438.
11. Bordenave, N.; Hamaker, B. R.; Ferruzzi, M. G. Nature and consequences of non-covalent interactions between flavonoids and macronutrients in foods. Food Funct. **2014**, 5, 18-34.
12. Escobar-Puentes, A. A.; Yobanny Reyes-Lopez, S.; Ruiz Baltazar, A. D. J.; Lopez-Teros, V.; Wall-Medrano, A. Molecular interaction of β-carotene with sweet potato starch: a bleaching-restitution assay. Food Hydrocoll. **2022**, 127, 107522.
13. Chai, Y.; Wang, M.; Zhang, G. Interaction between amylose and tea polyphenols modulates the postprandial glycemic response to high-amylose maize starch. J Agric Food Chem. **2013**, 61, 8608-8615.
14. Gao, Q.; Zheng, J.; Meeren, P.V.D.; Zhang, B.; Fu, X.; Huang, Q. A comparative study on stabilizing and releasing thymol by pre-formed V-type starch and β-cyclodextrin. Food Hydrocoll. **2024**, 156, 110233.
15. Chang, F.; He, X.; Huang, Q. Effect of lauric acid on the v-amylose complex distribution and properties of swelled normal cornstarch granules. Journal of Cereal Science **2013**, 58, 89-95.

 doi:10.20944/preprints202410.0484.v1

16. Liu, H.F.; Meng, P.; Zhang, Y.; Zheng, B.D.; Zeng H. L. Complexation of V-type lotus seed starch and butyric acid: Structure and in vitro digestion. Food Hydrocollo. **2024**, 149, 109527.
17. Xu, M.J., Saleh, A.S.M.; Gong, B.; Li, B.; Jing, L.; Gou, M.; Jiang, H.; Li. W.H. The effect of repeated versus continuous annealing on structural, physicochemical, and digestive properties of potato starch. Food Res Int. **2018**, 111, 324-333.
18. Zou, J.; Xu, M. J.; Tang, W.; Wen, L.R.; Yang, B. Modification of structural, physicochemical and digestive properties of normal maize starch by thermal treatment. Food Chem. **2019**, 309, 125733.
19. Zou, J.; Feng, Y.T.; Xu, M.J.; Yang, P.Y.; Zhao, X.D.; Yang, B. The structure-glycemic index relationship of Chinese yam (*Dioscorea opposita* thunb.) starch. Food Chem. **2023**, 421, 136228.
20. Gong, B.; Xu, M.J.; Li, B.; Wu, H.; Liu, Y.; Zhang, G.; Ouyang, S.H.; Li, W.H. Repeated heat-moisture treatment exhibits superiorities in modification of structural, physicochemical and digestibility properties of red adzuki bean starch compared to continuous heat-moisture way. Food Res Int. **2017**, 102, 776.
21. Gayary, M.A.; Marboh, V.; Mahnot, N. K., Chutia, H.; Mahanta, C. L. Characteristics of rice starches modified by single and dual heat moisture and osmotic pressure treatments. Int J Biol Macromol. **2024**, 255, 127932.
22. Van Soest J.J.G.; Tournois, H.; De Wit, D.; Vliegenthart, J.F.G. Short-range structure in (partially crystalline potato starch determined with attenuated total reflectance Fourier-transform IR spectroscopy. Carbohyd Res. **1995**, 279, 201-214.
23. Xu, H.; Hao, Z.; Zhang, J. Influence pathways of nanocrystalline cellulose on the digestibility of corn starch: gelatinization, structural properties, and a-amylase activity perspective. Carbohyd Polym. **2023**, 314, 120940.
24. Morgan, K. R.; Furneaux, R. H.; Stanley, R. A. Observation by solid-state 3C CP MAS NMR spectroscopy of the transformations of wheat starch associated with the making and staling of bread. Carbohyd Polym. **1992**, 235, 15-22.
25. Ma, Z.; Boye, J. I. Research advances on structural characterization of resistant starch and its structure-physiological function relationship: A review. Critical Crit Rev Food Sci. **2018**, 58, 1059-1083.
26. Bogracheva, T.Y.; Wang, Y. L.; Hedley, C. L. The effect of water content on the ordered/disordered structures in starches. Biopolymers **2015**, 58, 247-259.
27. Li, H.; Thuy Ho, V. T.; Turner, M. S.; Dhital, S. Encapsulation of Lactobacillus plantarum in porous maize starch. LWT-Food Science and Technol. **2016**, 74, 542-549.
28. Shi, M.M.; Song, X.; Chen, J.; Ji, X.L.; Yan, Y.Z. Effect of Oat Beta-Glucan on Physicochemical Properties and Digestibility of Fava Bean Starch. Foods **2024**, 13, 2046.
29. Zheng, Y.X.; Chen, S.Y.; Hu, Y.Y.; Ye, X.Q.; Wang, S.Y.; Tian, J.H. The cooperation of maize starch and ferulic acid under different treatments and its effect on postprandial blood glucose level, Food Hydrocoll. **2024**, 27, 110361.
30. Dhital, S.; Shrestha, A. K.; Gidley, M. J. Relationship between granule size and in vitro digestibility of maize and potato starches. Carbohyd Polym. **2010**, 82, 480-488.
31. Yao, T.; Sui, Z.; Janaswamy, S. Complexing curcumin and resveratrol in the starch crystalline network alters in vitro starch digestion: towards developing healthy food materials. Food Chem. **2023**, 425, 136471.
32. Mani, R.; Bhattacharya, M. Properties of injection moulded starch/synthetic polymer blends-iii. effect of amylopectin to amylose ratio in starch. Eur Polym J. **1998**, 34, 1467-1475.
33. Chen, L.; Ma, R.; Zhang, Z.; Mcclements, D.J.; Tian, Y. Impact of frying conditions on hierarchical structures and oil absorption of normal maize starch. Food Hydrocoll. **2019**, 97, 105231.
34. Zhou, X.; Chang, Q.; Li, J.; Jiang, L.; Jin, Z. Preparation of V-type porous starch by amylase hydrolysis of V-type granular starch in aqueous ethanol solution. Int. J. Biol. Macromol. **2021**, 183, 890-897.
35. Wang, Q.L.; Yang, Q.; Kong, X.P.; & Chen, H. Q. The addition of resistant starch and protein to the batter reduces oil uptake and improves the quality of the fried batter-coated nuts. Food Chem. **2024**, 438, 137992.
36. Ziaiifar, A.M.; Achir, N.; Courtois, F.; Trezzani, I.; Trystram, G. Review of mechanisms, conditions, and factors involved in the oil uptake phenomenon during the deep-fat frying process. Int J Food Sci Tech. **2008**, 43, 1410-1423.

 doi:10.20944/preprints202410.0484.v1

37. Salehi, F. Color changes kinetics during deep fat frying of kohlrabi (Brassica oleracea var. gongylodes) slice. Int J Food Prop. **2019**, 22, 511-519.
38. Lisiecka, K.; Wójtowicz, A.; Samborska, K.; Mitrus, M.; Oniszczuk, T.; Combrzyński, M.; Soja, J.; Lewko, P.; Drozd, K.K.; Oniszczuk, A. Structure and texture characteristics of novel snacks expanded by various methods. Materials **2023**, 16, 1541.